

# Synthesis of positively and negatively charged silver nanoparticles and their deposition on the surface of titanium

A Sharonova<sup>1</sup>, K Loza<sup>2</sup>, M Surmeneva<sup>1</sup>, R Surmenev<sup>1</sup>, O Prymak<sup>2</sup> and M Epple<sup>2</sup>

<sup>1</sup> National Research Tomsk Polytechnic University, Tomsk, Russia

<sup>2</sup> University of Duisburg-Essen, Essen, Germany

E-mail: rsurmenev@mail.ru

**Abstract.** Bacterial infections related to dental implants are currently a significant complication. A good way to overcome this challenge is functionalization of implant surface with Ag nanoparticles (NPs) as antibacterial agent. This article aims at review the synthesis routes, size and electrical properties of AgNPs. Polyvinyl pyrrolidone (PVP) and polyethyleneimine (PEI) were used as stabilizers. Dynamic Light Scattering, Nanoparticle Tracking Analysis, X-ray diffraction (XRD), scanning electron microscopy (SEM), and energy dispersive spectroscopy (EDX) have been used to characterize the prepared AgNPs. Two types of NPs were synthesized in aqueous solutions: PVP-stabilized NPs with a diameter of the metallic core of  $70 \pm 20$  nm, and negative charge of  $-20$  mV, PEI-stabilized NPs with the size of the metallic core of  $50 \pm 20$  nm and positive charge of  $+55$  mV. According to SEM results, all the NPs have a spherical shape. Functionalization of the titanium substrate surface with PVP and PEI-stabilized AgNPs was carried out by dropping method. XRD patterns revealed that the AgNPs are crystalline with the crystallite size of 14 nm.

## 1. Introduction

Metals have a long history in the treatments of dentistry and orthopedics. Pure titanium is commonly used as artificial joints and implants in both dental and orthopedic clinics because of its biocompatibility and mechanical properties. A major factor that determines the success of dental implantation is osseointegration, which is the stable anchorage of an implant in living bone achieved by direct bone-to-implant contacts [1, 2]. It is commonly known that the implantation of a foreign object into the human body may be rejected. Moreover, a wide range of local tissue reactions, in particular inflammation, giant cell formation and fibrosis can be induced [3]. A promising solution to this problem is formation of an antibacterial bioactive coating on the implant surface, which allows to avoid rejection and speed up the treatment and recovery process [4, 5].

The consequences of implant-associated infection are significant and usually require revision surgery, with removal of the implant and prolonged antibiotic treatment. Various approaches have been investigated to reduce the rate of infection. Two recent strategies are the coating of implants with antibiotics and followed by covalently attaching of antimicrobial nanoparticles to the implant surface. The remarkable mechanism of the antimicrobial activity of Ag nanoparticles (AgNPs) is related to the formation of free radicals and consequent free-radical-induced oxidative damage of the cell membranes of bacteria [6, 7]. The purpose of these bioactive surfaces is to disrupt the metabolic machinery of the microbes or to prevent bacterial adhesion to the implant and, consequently, the development of biofilm [8].



Currently, many methods have been reported for the synthesis of AgNPs by using chemical [9-11], physical [12, 13], photochemical [14, 15] and biological [16-18] routes. Each method has advantages and disadvantages with the common challenges such as production costs, scalability, particle sizes and size distribution. Among the existing methods, the chemical methods have been mostly used for production of AgNPs. Chemical methods provide an easy way to synthesize AgNPs in solution.

A vast number of nanoparticle systems have been reported to be used to prepare highly stable Ag NPs, based on various groups that are capable of binding to metal surfaces: phosphonic acid [19], aminocellulose as a combined reducing and capping reagent [20]. Useful coatings for biomedical application and delivery of AgNPs, based on glutathione, thiols, disulfides, thioethers, thioesters, thiocarbonates, and thiocarbamates are used in the preparation of metal nanoparticles [21]. Poly(vinylpyrrolidone) (PVP) and poly(ethylenimine) (PEI)-stabilized AgNPs are stable in suspension and exhibit little change in size or electrophoretic mobility [22, 23].

The purpose of this study is to find appropriate parameters of AgNPs such as size,  $\zeta$  - potential, charge for the deposition on metallic substrates. These parameters of AgNPs are important for the development of the structure of scaffolds.

## 2. Materials and methods

### 2.1. Samples preparation

To prepare the samples as substrates commercially pure titanium (99.58 wt% titanium; 0.1 wt% oxygen; 0.15 wt% iron; 0.05 wt% carbon; 0.04 wt% nitrogen; 0.08 wt% silicon) plates (10×10 mm) were used. The plates were chemically etched in acid solution containing HF (48%) and HNO<sub>3</sub> (66%) dissolved in the distilled water with the ratio 1:2:2.5 in volume. After acid etching, the samples were ultrasonically washed sequentially in ethanol and deionized water for 10 minutes at room temperature.

### 2.2. The synthesis of positively and negatively charged AgNPs

The negatively charged AgNPs were synthesized by wet chemical reduction method of silver nitrate (Fluka, p.a.) using glucose (D-(+)-glucose, Baker) as a reductant and polyvinylpyrrolidone (PVP K30 Povidon 30; Fluka, molecular weight 40000 g mol<sup>-1</sup>) as a stabilizer. 2 g glucose and 1 g PVP were dissolved in 40 g water and heated to 90 °C. Then 0.5 g AgNO<sub>3</sub> dissolved in 1 mL water was quickly added. The synthesis of positively charged, PEI-stabilized, AgNPs was proceeded without use of glucose. The 1g polyethylenimine (PEI; branched, Aldrich, molecular weight 25 000 g mol<sup>-1</sup>) was dissolved in 40 g water and heated to 90°C. Then 0.5 g AgNO<sub>3</sub> dissolved in 1 mL water was quickly added. The dispersion was kept at 90 °C for 1 h, PVP-stabilized AgNPs and then left to cool to room temperature. The particles were collected by ultracentrifugation (3 times, 30 000 rpm, 30 min), redispersed in pure water and collected again by ultracentrifugation. Thereby NO<sub>3</sub><sup>-</sup>, excess glucose and its oxidation products, excess PVP/PEI, and excess Ag<sup>+</sup> were removed. The silver nanoparticles were further redispersed in water.

### 2.3. Characterization of AgNPs

The hydrodynamic diameter (HDD) of the AgNPs were measured by Dynamic Light Scattering (DLS) using a Malvern Zetasizer Nano ZS and Nanoparticle Tracking Analysis (NTA) using a NanoSight LN 10. Zeta ( $\zeta$ ) potential of the AgNPs were measured by DLS. Both of these methods are based on the rate of Brownian motion to particle size and applicable to analyse the particles of a diameter 10-2000 nm in liquids. DLS technique is used to measure the diffusion of particles and converts this to the size and a size distribution using the Stokes-Einstein relationship. Non-invasive back scatter technology is used to give the highest sensitivity simultaneously with the highest size and concentration range. NTA is a unique method for visualisation. The light scattered by the particles is captured using a scientific digital camera and the motion of each particle is tracked from the frame to frame by the specially developed software. This rate of particles movement is related to a sphere equivalent hydrodynamic

radius as calculated through the Stokes-Einstein equation [24-26]. By scanning electron microscopy (SEM) the morphology and size of the AgNPs were estimated using an ESEM Quanta 400 FEG instrument operating in a high vacuum with gold/palladium-sputtered samples. The Grazing-incidence small-angle X-ray scattering (GISAXS) was used to determine the internal structure of studied AgNPs. The phase parameters of AgNPs were investigated by the method of X-ray diffraction in the Bragg-Brentano geometry (Siemens Diffractometer D500), in a direction perpendicular to the diffraction plane, calculated according to the Scherrer Equation [27]:

$$R_{hkl} = k \cdot \lambda (\beta \cdot \cos \theta)^{-1}, \quad (1)$$

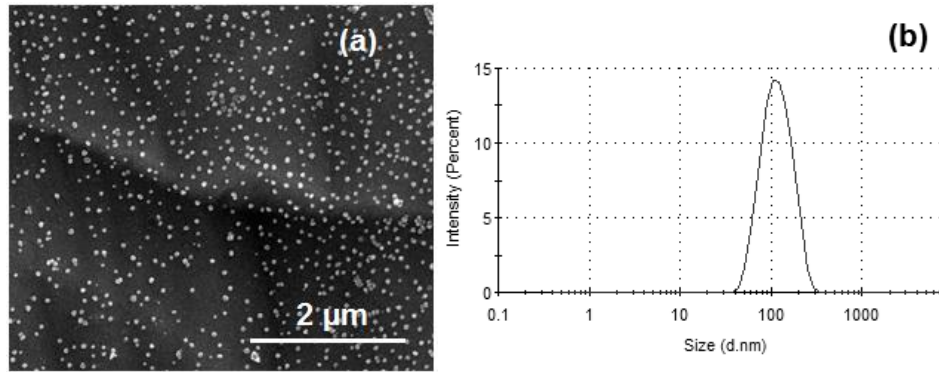
where,  $R_{hkl}$  - crystallite size in the direction perpendicular to the diffraction plane  $hkl$ ;  $k = 0.9$ ,  $\lambda$  - wavelength of the analyzing X-ray beam;  $\theta$  - angle subtended by the diffraction,  $\beta = B_{1/2} - b_{1/2}$  - the true width of the line;  $B_{1/2}$  and  $b_{1/2}$  - experimental and instrumental broadening of the width of the diffraction peak at half intensity.

#### 2.4. Dropping method of AgNPs deposition

The deposition of PVP and PEI stabilized AgNPs on titanium substrate was done by dropping method. The process of dropping method based on formation of a drop 120  $\mu\text{L}$  of the working solution with the concentration 60  $\mu\text{g}/\text{mL}$  and following drying at 55.5°C.

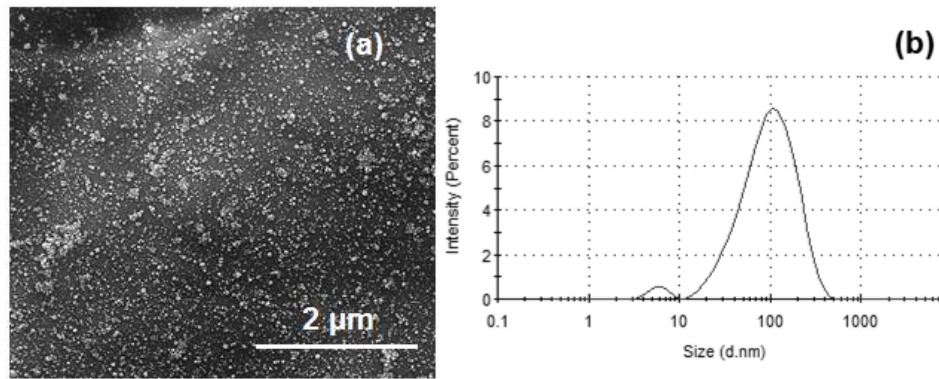
### 3. Results and discussions

Table 1 contains information about the diameter of the metallic core, HDD as determined through DLS, the PDI and  $\zeta$ -potential. The HDD,  $\zeta$ -potential and polydispersity index (PDI) of the nanoparticles were measured by DLS using a Malvern Zetasizer Nano ZS. The results of DLS analysis revealed that PVP-stabilized AgNPs had the  $\zeta$ - potential of -20 mV, average HDD of 110 nm and PDI of -0.195, indicating the absence of large agglomerates and presence of a monodisperse system. Figure 1 illustrated the data describing PVP-stabilized AgNPs with the dispersion time 1 hour. The SEM analysis confirmed the ability to attain a uniform distribution of AgNPs. Thus, SEM images showed that the PVP-stabilized AgNPs had a spherical shape with a diameter of the metallic core of  $70 \pm 20$  nm. It is reported [28] that silver nanoparticles (PVP-stabilized, 70 nm) affected the viability of *Staphylococcus aureus* colonies. The antimicrobial activity of silver nanoparticles was tested using standard methods which determine the minimum inhibitory concentration (MIC) and the minimum bactericidal concentration (MBC). *S. aureus* ( $10^6$  cells  $\text{mL}^{-1}$  in medium) was treated without (*S. aureus* in pure medium: positive control; pure medium: negative control) or with 50 mg/mL or 30 mg/mL of silver nanoparticles for 24 h under cell culture conditions. Subsequently, the bacteria were plated and incubated for further 24 h at 37 °C on blood agar plates. From the reported experiments and the available literature on the dissolution of silver nanoparticles, they conclude that the particles will dissolve after coming into contact with air, therefore they will become increasingly bactericidal (and cytotoxic) with time.



**Figure 1.** a) SEM image of PVP-stabilized AgNPs, b) DLS estimated distribution size of AgNPs.

The results of DLS analysis of PEI-stabilized AgNPs showed the  $\zeta$ -potential of +55 mV, average HDD of 110 nm (figure 2). The PDI for PVP-stabilized AgNPs was lower than 0.3, which could indicate that system was monodisperse, however, PDI in case of PEI-stabilized AgNPs was slightly more than 0.3. Moreover, according to DLS of AgNPs obtained using PEI had a multidistribution. Typical SEM image of AgNPs with spherical shape was shown in figure 2. Zhiguo Liu et al. [29] showed that the PEI-functionalized Ag nanoparticles were positively charged. Moreover, the Ag colloids exhibited stronger antibacterial activity in the bactericidal test. Its bactericidal efficiency exceeds the commonly used antibacterial agents such as Erythromycin, chloramphenicol and penicillin as well as AgNO<sub>3</sub> solution. These results prove that our synthesis method is efficient to produce a stable PEI-functionalized Ag colloid with excellent antibacterial activity.



**Figure 2.** a) SEM image of PEI-stabilized AgNPs, b) DLS estimated distribution size of AgNPs.

Negatively charged AgNPs are monodisperse and have a narrow size distribution. These properties of AgNPs are prospective to develop antibacterial layers on implant surfaces.

**Table 1.** The properties of silver nanoparticles stabilized with PEI and PVP polymer.

Polymer	Diameter, nm			PDI	$\zeta$ -potential, mV
	NTA	DLS	SEM		
PVP	115	110	70	0.195	-20
PEI	30	110	50	0.404	+55

To form an antibacterial interface of metal implant the dropping method was used (120  $\mu$ L with concentration 60  $\mu$ g/mL).

The patterns of AgNPs distribution on titanium surface substrate are shown in figure 3.

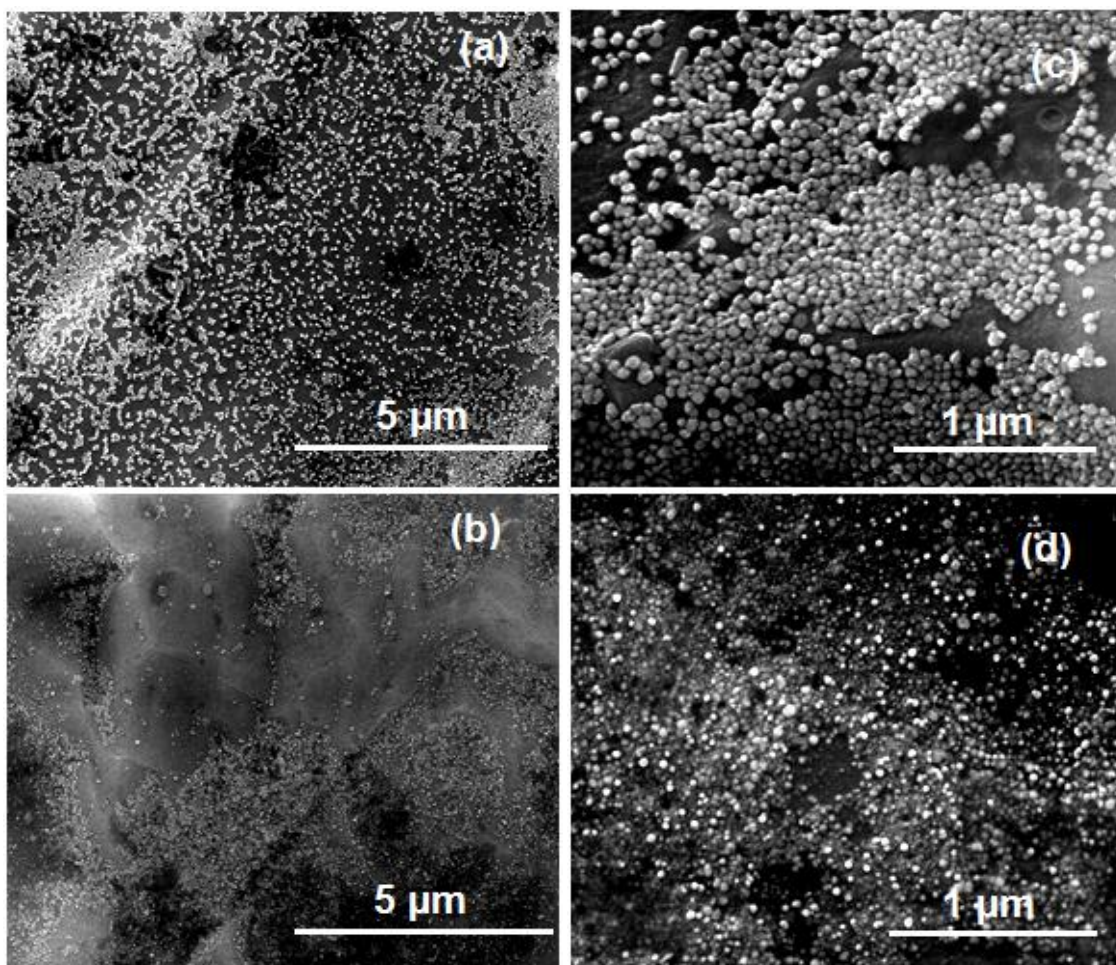


**Figure 3.** SEM images distribution of AgNPs on the surface of pure titanium by drop method (120  $\mu\text{L}$  with concentration 60  $\mu\text{g/mL}$ ) stabilized with a), c) PVP and b), d) PEI.

SEM images revealed that the both types of AgNPs have a spherical shape (figure 3). PVP-stabilized AgNPs were homogeneously distributed over the entire surface. Dropping method has the disadvantage associated with the surface tension and as a consequence the samples are not fully covered by the particles. The particle size of PEI-stabilized AgNPs was smaller than PVP-stabilized AgNPs as it could be seen from the obtained data (Table. 1). In case of positively charged AgNPs the dropping method does not allow a complete and homogeneous coverage of the sample surface. The negatively charged AgNPs were used to create a homogeneous layer of AgNPs on the surface of titanium without any agglomeration. Negatively charged AgNPs were studied by XRD to reveal their structure parameters. In figure 4 and Table 2 the typical XRD patterns are presented.

XRD pattern of AgNPs on the titanium substrate showed the presence of reflexes at 2 Theta angles of  $44.3^\circ$  and  $77.3^\circ$ , which can be indexed to (200) and (311) planes of pure silver (PDF # 04-0783). Since the main reflection of titanium and silver were very close it was decided to use a silicon substrate as a control the presence of silver.

The typical XRD pattern, which illustrates the formation of intense lines of reflection of the Ag, is shown on silicon substrate (figure 4). The presence of peaks at 2  $\theta$  values  $38.1^\circ$ ,  $44.3^\circ$ ,  $64.4^\circ$  and  $77.3^\circ$  corresponded to (111), (200), (220), and (311) planes of silver, respectively. Thus, the XRD pattern

confirmed the cubic crystalline structure of silver (JCPDS, 4-0783). The lattice constants calculated from XRD pattern of PVP and PEI-stabilized NPs were found to be  $a=4.093 \text{ \AA}$  and  $4.085 \text{ \AA}$ , correspondently. The crystallite size of AgNPs was found to be 14 and 13 nm in the case of titanium and silicon substrate, respectively (Table 2). The aim of the developed biocomposite is a long-term antibacterial protection against implant associated infections.

**Table 2.** The lattice parameters and crystallite size of AgNPs on titanium and silicon substrate.

Sample	Lattice parameters		Crystallite size, nm
	$a=b, \text{ \AA}$	$V, \text{ \AA}^3$	
Titanium	4.093	68.52	14
Silicon	4.085	68.22	13

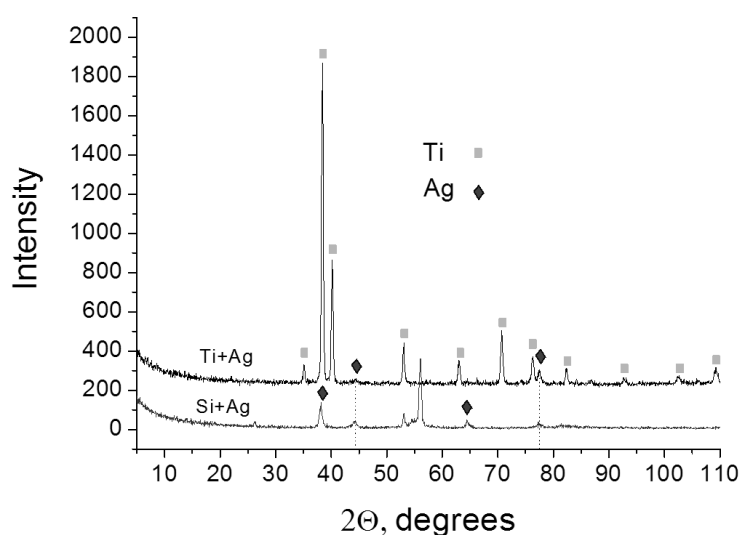


**Figure 4.** The XRD patterns of AgNPs deposited by dropping method (120  $\mu\text{L}$  with concentration 60  $\mu\text{g/mL}$ ) on titanium and silicon substrates.

#### 4. Conclusions

In this study two types of AgNPs were synthesized: PVP-stabilized negatively charged ( $-20 \text{ mV}$ ) nanoparticles with the size of  $70 \pm 20 \text{ nm}$  and PEI-stabilized positively charged ( $+55 \text{ mV}$ ) nanoparticles with the size of  $50 \pm 20 \text{ nm}$ . According to the SEM data, all the particles had a spherical shape. The dropping method was used for AgNPs deposition on titanium substrate. It was revealed that the dropping method did not allow to get a homogeneous layer of nanoparticles in case of the PVP-stabilized AgNPs. In contrast with the PVP-stabilized AgNPs, the uniform layer of PEI-stabilized AgNPs was formed. No agglomeration of AgNPs after deposition on the titanium substrate was observed. The XRD data obtained for the PVP-stabilized AgNPs on Ti substrate showed the typical peaks of Ag at 2 Theta angles of  $44.3^\circ$  and  $77.3^\circ$  with the coherent scattering region of 14 nm.

#### References

- [1] Hanawa T 2010 *Japanese Dental Science Review. Series* **46** pp 93–101
- [2] Guo C Y, Matinlinna J P and Tang A T H 2012. *Int. J. Biomater.* **2012** 381535
- [3] IARC Working Group on the Evaluation of Carcinogenic Risks to Humans 1990 *Surgical implants and other foreign bodies* (Lyon: IARC Press)

- [4] Lilja M. 2013 *Bioactive Surgical Implant Coatings with Optional Antibacterial Function Digital Comprehensive Summaries of Uppsala Dissertations from the Faculty of Science and Technology 1091* (Room: Acta Universitatis Upsaliensis)
- [5] Farooq I, Irman Z, Farooq U, Leghari A, Ali U. 2012 Bioactive Glass: A Materials for the Future *World Journal of dentistry* **3** 199–201
- [6] Gupta K, Singh R. P., Pandey A, Pandey A 2013 Photocatalytic antibacterial performance of TiO<sub>2</sub> and Ag-doped TiO<sub>2</sub> against *S. aureus*, *P. aeruginosa* and *E. coli* *Beilstein J. Nanotechnol.* **4** 345–351
- [7] Hwang E T, Lee J H, Chae Y J, Kim Y S, Kim B C, Sang B I, Gu M B 2008 Analysis of the toxic mode of action of silver nanoparticles using stress-specific bioluminescent bacteria *Small* **4** 746–50
- [8] Ketonis C, Parvizi J, Jones L C 2012 Evolving Strategies To Prevent Implant-associated Infections *JAAOS* **20** 478–80
- [9] Chen S, Zhang H, 2012 Aggregation kinetics of nanosilver in different water conditions *Adv. Nat. Sci.: Nanosci. Nanotechnol.* **3** 035006
- [10] Dang T M D, Le T T T, Fribourg-Blanc E, Dang M C 2012 Influence of surfactant on the preparation of silver nanoparticles by polyol method *Adv. Nat. Sci.: Nanosci. Nanotechnol.* **3** 035004
- [11] Patil R S, Kokate M R, Jambhale C L, Pawar S M, Han S H, Kolekar S S 2012 One-pot synthesis of PVA-capped silver nanoparticles their characterization and biomedical application *Adv. Nat. Sci.: Nanosci. Nanotechnol.* **3** 015013
- [12] Siegel J, Kvítek O, Ulbrich P, Kolská Z, Slepíčka P, Švorčík V 2012 Progressive approach for metal nanoparticle synthesis *Mater. Lett.* **89** 47–50
- [13] Tseng K, Lee H, Liao C, Chen K, Lin H 2013 Rapid and Efficient Synthesis of Silver Nanofluid Using Electrical Discharge Machining *J. of Nanomater.* **2013** 174939
- [14] Christy A J, Umadevi M 2012 Synthesis and characterization of monodispersed silver nanoparticles *Adv. Nat. Sci.: Nanosci. Nanotechnol.* **3** 035013
- [15] Sakamoto M, Fujistuka M, Majima T 2009 Light as a construction tool of metal nanoparticles: synthesis and mechanism *J. Photochem. Photobiol. C* **10** 33–56
- [16] Sintubin L, Verstraete W, Boon N 2012 Biologically produced nanosilver: Current state and future perspectives *Biotechnol. Bioeng.* **109** 2422–36
- [17] Amaladhas T P, Sivagami S, Devi T A, Ananthi N, Velammal S P 2012 Biogenic synthesis of silver nanoparticles by leaf extract of *Cassia angustifolia* *Adv. Nat. Sci.: Nanosci. Nanotechnol.* **3** 045006
- [18] Umadevi M, Shalini S, Bindhu M R 2012 Synthesis of silver nanoparticle using *D. carota* extract *Adv. Nat. Sci.: Nanosci. Nanotechnol.* **3** 025008
- [19] Chaikin Y, Bendikov T A, Cohen H, Vaskevich A, Rubinstein I 2013 Phosphonate-stabilized silver nanoparticles: One-step synthesis and monolayer assembly *J. Mater. Chem. C* **1** 3573–83
- [20] Cheng F, Betts J W, Kelly S M, Schaller J, Heinze T 2013 Synthesis and antibacterial effects of aqueous colloidal solutions of silver nanoparticles using aminocellulose as a combined reducing and capping reagent *Green Chem.* **15**, 989–98
- [21] Taglietti A, Diaz Fernandez Y A, Amato E, Cucca L, Dacarro G, Grisoli P 2012 Antibacterial activity of glutathione-coated silver nanoparticles against Gram positive and Gram negative bacteria *Langmuir* **28** 8140–48
- [22] Römer I, White T A, Baalousha M, Chipman K, Viant M R, Lead J R 2011 Aggregation and dispersion of silver nanoparticles in exposure media for aquatic toxicity tests *J. Chromatogr. A* **1218** 4226–33
- [23] Kima K, Lee H B, Lee J W, Shin K S 2010 Poly(ethylenimine)-stabilized silver nanoparticles assembled into 2-dimensional arrays at water–toluene interface *J. Colloid Interface Sci.* **345** 103–108

- [24] Chuaha L H, Roberts C J, Billac N, Abdullah S, Roslid R, Manickame S, 2014 Using Nanoparticle Tracking Analysis (NTA) to Decipher Mucoadhesion Propensity of Curcumin-Containing Chitosan Nanoparticles and Curcumin Release *J. Dispersion Sci. Technol.* **35** 1201–07
- [25] Arzensek D 2010 *Dynamic light scattering and application to proteins in solutions* (Ljubljana: University of Ljubljana Faculty of Mathematics and Physics)
- [26] Frisken, Barbara J 2001 Revisiting the Method of Cumulants for the Analysis of Dynamic Light-Scattering Data *Appl. Opt.* **40** 4087–91
- [27] Surmenev R A, Surmeneva M A, Pichugin V F, Epple M 2009 RF-magnetron calcium phosphate coatings on materials medical implants *Bulletin of the Tomsk Polytechnic University* **315** 138–141.
- [28] Loza K, Diendorf J, Sengstock C, Ruiz-Gonzalez L, Gonzalez-Calbet J M, Vallet-Regi M, Koller M, Epple M 2014 The dissolution and biological effects of silver nanoparticles in biological media *Cite this: J. Mater. Chem. B* **2** 1634–43
- [29] Liu Z, Wang Y, Zu Y, Fu Y, Li N, Guo N, Liu R, Zhang Y 2014 Synthesis of polyethylenimine (PEI) functionalized silver nanoparticles by a hydrothermal method and their antibacterial activity study *Mater Sci Eng C Mater Biol Appl.* **42** 31–37
- [30] Ivanova A A, Surmenev R A, Surmeneva M A, Mukhametkaliyev T, Sharonova AA, Grubova I Yu, Loza K, Chernousova S, Prymak O, Epple M, 2014 Antibacterial AgNPs/CaP biocomposites *CUET* **2014** 472–474